

SOLAR RADIATION FORCE MODELING FOR TDRS ORBIT
DETERMINATION*

Taesul Lee, Michael J. Lucas, and Robert E. Shanklin, Jr.

Computer Sciences Corporation

ABSTRACT

The relative orbit determination accuracies resulting from several TDRS models used for solar radiation force calculations are evaluated. These models include spherical, single-plate, and restricted two-plate models. The plate models can be adjusted in both area and reflectivity through differential correction. The restricted two-plate model has an Earth-pointing plate and a solar plate; the orientation of the solar plate is restricted to rotation about an axis perpendicular to the satellite's orbital plane.

Simulated TDRS observations are generated from an ephemeris obtained using a 69-component TDRS model. These observations are processed by least squares differential correction in order to find optimized parameters for the spherical, single-plate, and multi-plate models. The solutions for the parameters and the state vector are then used to generate ephemerides that are compared with the 69-component ephemeris to estimate the expected orbit determination accuracies achievable with the various TDRS models.

*This work was supported by the Operations Analysis Section, Operational Orbit Support Branch, Goddard Space Flight Center, National Aeronautics and Space Administration, under Contract NAS 5-24300.

SECTION 1 - INTRODUCTION

A study of the solar radiation pressure (SRP) effect on orbit determination for a Tracking and Data Relay Satellite (TDRS) has been carried out using simulated data. The TDRS System consists of three geosynchronous satellites--TDRS East, TDRS West, and TDRS Spare--and one common ground tracking facility. These satellites will be placed in circular, nearly equatorial orbits at a height of 36,000 kilometers above the surface of the Earth. The study is designed to determine whether a complex SRP model for a TDRS can be satisfactorily replaced by a simpler SRP model, such as a constant-effective-area model or a two-plate model. In addition, different tracking station configurations are used to investigate the possible dependence of the results on the tracking station geometry.

A similar study carried out by Chan et al. (Reference 1) used a 69-component TDRS SRP model and a two-plate model with four adjustable parameters. The adjustable parameters were determined by using a least squares procedure to minimize the position differences between two ephemerides, one obtained using the 69-component model and one obtained using the two-plate model.

Another investigation related to the present study was carried out by Shanklin et al. (Reference 2) in which a constant-effective-area SRP model and a two-plate model were compared using real ATS-6 S-Band tracking data. This study, however, was somewhat incomplete due to the limited availability of ATS-6 tracking data. The current study is an extension of that work and follows the same approach as that used in Reference 1 in constructing the TDRS SRP models. The current study, however, uses simulated bilateration and S-Band tracking data in the differential correction process

instead of position differences between the two ephemerides as used by Chan.

The study plan is as follows. First, a 69-component SRP model of a TDRS, which is available in the Research and Development version of the Goddard Trajectory Determination System (RDGTDS), is used to compute a truth ephemeris, which is subsequently used to generate various types of simulated observations using the Mission Data Generation System (MDGS). The MDGS produces raw data in a 75-byte format, and the Generalized Data Handler (GDH) converts these raw data into the 60-byte format for the Goddard Trajectory Determination System (GTDS). Second, these simulated data are used in regular GTDS Differential Correction (DC) Program runs to find optimized SRP parameters for the constant-effective-area model and for the two-plate model. The constant-effective-area model contains one adjustable parameter, and the two-plate model contains four adjustable parameters. Any combination of the four parameters of the two-plate model can be solved for in a given DC Program run. Third, ephemerides are generated using the final elements and SRP parameters obtained from the DC Program runs, and these ephemerides are then compared with the original truth ephemeris.

Brief descriptions of the TDRS solar radiation pressure models are given in Section 2 and generation of the simulated data is discussed in Section 3. The results of various DC Program runs and ephemeris comparisons are presented in Section 4, and the conclusions are summarized in Section 5.

SECTION 2 - DESCRIPTION OF MODELS

The 69-component model is composed of 69 distinctive parts. The components with relatively large areas are the two solar panels, whose normals make minimum angles with the satellite-Sun line; the antennas; the antenna feeds; and the top, bottom, and six sides of the main body (see Reference 1 for details).

The simplest SRP model used to approximate the 69-component model is the constant-effective-area model. In this model, the area for the SRP calculation is assumed to be constant and always normal to the satellite-Sun line. The force due to the solar radiation pressure (Reference 3) is given by

$$\vec{f}_{\text{SRP}} = -v a P (1 + \eta) \vec{u}_{\text{Sun}} \quad (2-1)$$

where v = eclipse factor
 a = constant area
 P = solar radiation pressure on a perfectly absorbing surface at the position of the satellite
 η = surface reflectivity
 \vec{u}_{Sun} = unit vector along the satellite-Sun line

The solar radiation pressure is inversely proportional to the square of the distance from the Sun, and the eclipse factor, v , equals zero if the satellite is in the Earth's shadow and equals one if it is not. The right-hand side of Equation (2-1) represents the sum of two parts: the part due to the absorption of the solar radiation, which is proportional to $(1 - \eta)$, and the part due to the reflected radiation, which is proportional to 2η . This model is currently available in GTDS.

The second model used to approximate the 69-component model is a two-plate model, which has an Earth-pointing plate and

a solar plate. The solar plate is hinged along an axis normal to the satellite's orbital plane and is always rotated about that axis so as to maximize the amount of sunlight falling on the plate. The force due to the solar radiation pressure for the two-plate model is given by the sum of four terms:

$$\begin{aligned}
 \vec{f}_{SRP} = & -aP[2\alpha_E \eta_E |\vec{u}_{Sun} \cdot \vec{R}| (\vec{u}_{Sun} \cdot \vec{R}) \vec{R} \\
 & + \alpha_E (1 - \eta_E) |\vec{u}_{Sun} \cdot \vec{R}| \vec{u}_{Sun} \\
 & + 2\alpha_S \eta_S (\vec{u}_{Sun} \cdot \vec{N}_S)^2 \vec{N}_S \\
 & + \alpha_S (1 - \eta_S) (\vec{u}_{Sun} \cdot \vec{N}_S) \vec{u}_{Sun}]
 \end{aligned}
 \tag{2-2}$$

where

- a = reference area
- P = solar radiation pressure on a perfectly absorbing surface at the position of the satellite
- α_E = scale factor for the area of the Earth-pointing plate
- α_S = scale factor for the area of the solar plate
- η_E = reflectivity of the Earth-pointing plate
- η_S = reflectivity of the solar plate
- \vec{u}_{Sun} = unit vector along the satellite-Sun line
- \vec{R} = unit position vector of the satellite
- \vec{N}_S = unit vector normal to the sunny side of the solar plate

In Equation (2-2), the first term is due to the reflection by the Earth-pointing plate, the second term is due to the absorption by the Earth-pointing plate, the third term is due to the reflection by the solar plate, and the fourth term is due to the absorption by the solar plate. The two area scale factors, α_E and α_S , and the two reflectivities, η_E and η_S , are adjustable parameters. In a given DC Program

run, any combination or all of these four parameters can be solved for. Instead of α_E , η_E , α_S , and η_S , an alternative set of four parameters, ξ_1 , ξ_2 , ξ_3 , and ξ_4 , may also be defined (and solved for):

$$\xi_1 = \alpha_E \eta_E$$

$$\xi_2 = \alpha_E (1 - \eta_E)$$

$$\xi_3 = \alpha_S \eta_S$$

$$\xi_4 = \alpha_S (1 - \eta_S)$$

SECTION 3 - GENERATION OF SIMULATED DATA

Tracking data for this study were generated using a satellite ephemeris tape obtained from a special RDGTDS Program load module that contains a 69-component TDRS model for SRP evaluation. This ephemeris tape was used by the MDGS Program to generate a second tape of raw range and Doppler simulated data. This simulated data tape was used by the GDH Program to generate tracking data in a format appropriate for use in the GTDS two-plate load module. Two types of tracking data were generated in this manner: Applications Technology Satellite Ranging (ATSR) bilateration data and Unified S-Band (USB) two-way data.

3.1 ATSR BILATERATION DATA

ATSR bilateration data were generated using the ground station at White Sands, New Mexico, as the ATSR tracker and the ground stations at Mojave, California; Rosman, North Carolina; Madrid, Spain; Quito, Ecuador; and Santiago, Chile, as the ATSR ground transponders. Figure 1 shows the positions of these six sites in relation to the expected sub-satellite point for the relay satellite.

Using these five tracker/ground transponder pairs, tracking data with the following characteristics were produced:

- Frequency: 5600 MHz (C-Band)
- Primary frequency offset: 5.8875 MHz
- Transponder delay: 0.0 km
- Tracking mode: satellite-to-ground phase-locked transponder
- Major range tone/minor range tone: 100 kHz/8 Hz

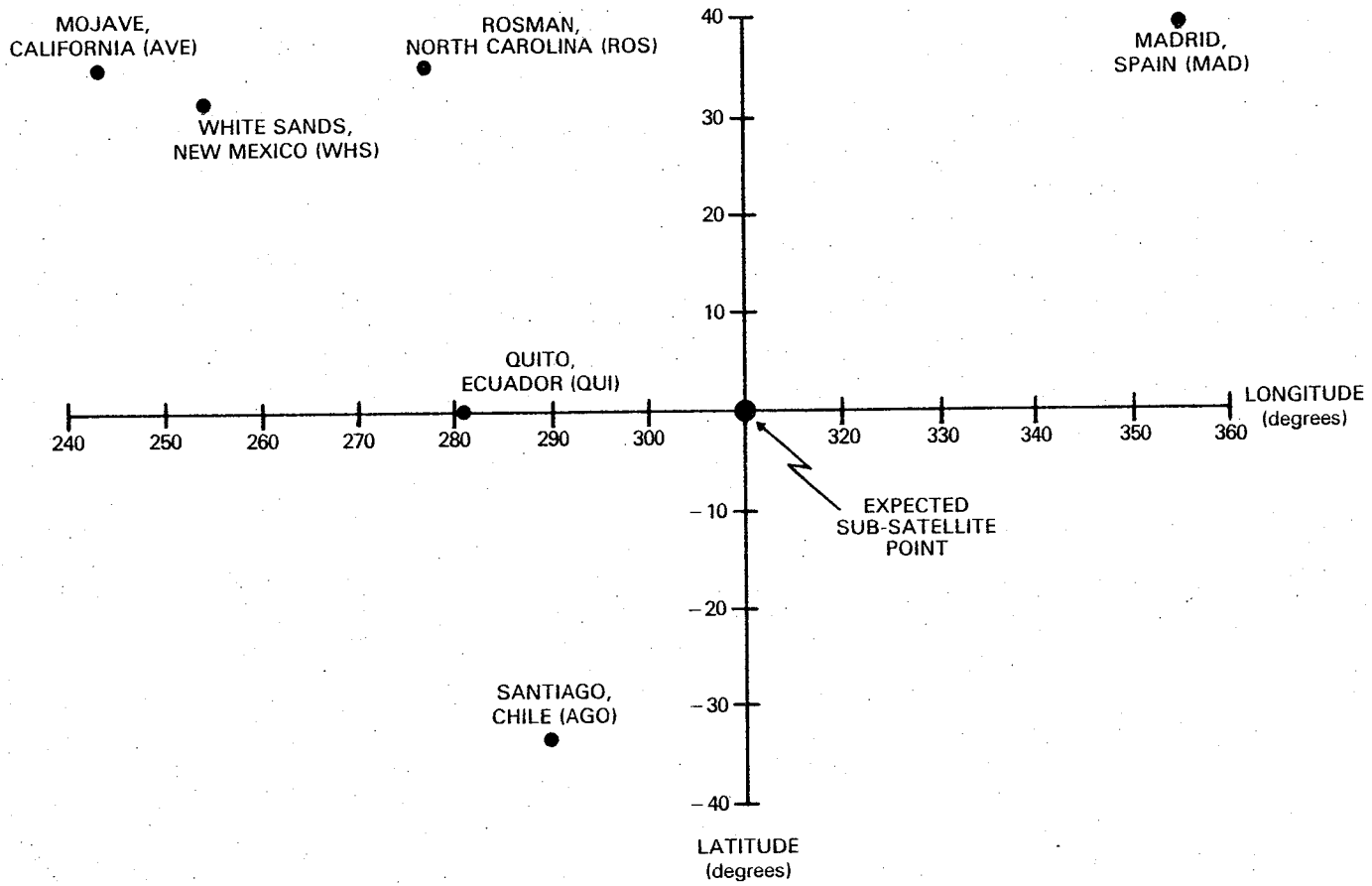


FIGURE 1. SITE LOCATIONS AND EXPECTED SUB-SATELLITE POINT

- Uplink pilot frequency/downlink pilot frequency:
6150 MHz/4150 MHz
- Doppler count mode: nondestruct

Data were produced at a rate of six observations per minute for the first 25 minutes of each hour, starting at 0.0 hours on October 2, 1980, and ending at 0.0 hours on October 3, 1980. Each tracker/ground transponder pair was enabled for tracking over the discrete time interval shown in Table 1. No observation corrections were applied and no observation noise was applied.

3.2 USB TWO-WAY DATA

USB two-way data (for which the receiving and transmitting sites are the same) were generated using the ground stations at Mojave, Rosman, Madrid, Quito, and Santiago. Tracking data with the following characteristics were produced:

- Transmit frequency: 2106 MHz
- Transponder delay: 0.0 km
- Ranging equipment: Spaceflight Tracking and Data Network (STDN) Ranging Equipment (SRE)
- Major range tone: 20 kHz

Data were produced for the first 25 minutes of each hour, over the same time period, at the same rate, and with the same corrections that were used for the ATSR bilateration data. Each ground station was enabled for tracking over the discrete time interval shown in Table 2.

**TABLE 1. TRACKING INTERVALS FOR ATSR TRACKER/
GROUND TRANSPONDER PAIRS**

| TRACKER/GROUND TRANSPONDER PAIR | MINUTES OF THE HOUR DURING WHICH THE PAIR IS ENABLED |
|------------------------------------|---|
| WHITE SANDS/ROSMAN | 00 TO 05 |
| WHITE SANDS/MOJAVE | 05 TO 10 |
| WHITE SANDS/QUITO | 10 TO 15 |
| WHITE SANDS/MADRID | 15 TO 20 |
| WHITE SANDS/SANTIAGO | 20 TO 25 |

8347/81

TABLE 2. TRACKING INTERVALS FOR USB GROUND STATIONS

| GROUND STATION | MINUTES OF THE HOUR DURING WHICH GROUND STATION IS ENABLED |
|-------------------|---|
| ROSMAN | 00 TO 05 |
| MOJAVE | 05 TO 10 |
| QUITO | 10 TO 15 |
| MADRID | 15 TO 20 |
| SANTIAGO | 20 TO 25 |

SECTION 4 - DIFFERENTIAL CORRECTION SOLUTIONS AND EPHEMERIS COMPARISON RESULTS

Differential correction solutions were obtained using different SRP models, different types of simulated observations, and different tracking station configurations.

4.1 RESULTS OBTAINED USING BILATERATION DATA AND TWO GROUND TRANSPONDERS

The results of DC Program solutions obtained using bilateration range and Doppler data and five different combinations of solve-for parameters in the two-plate model are presented in Tables 3 and 4. The simulated bilateration data used were obtained using the TDRSS ground station at White Sands and two ground transponders at Rosman, North Carolina, and Mojave, California. The five different SRP options used were

- Constant-effective-area model with C_R solved for
- Two-plate model with α_E and α_S solved for
- Two-plate model with ξ_1 and ξ_2 solved for
- Two-plate model with ξ_3 and ξ_4 solved for
- Two-plate model with ξ_1 , ξ_2 , and ξ_3 solved for

The third option, in which ξ_1 and ξ_2 are solved for, is equivalent to solving for α_E and η_E , the scale factor and reflectivity of the Earth-pointing plate, respectively. Similarly, the fourth option is equivalent to solving for α_S and η_S . In this particular set of DC Program runs, the values of the SRP parameters in the two-plate model that were not solved for were set equal to zero. Thus, the third and fourth options discussed above actually represent single-plate models rather than two-plate models.

An identical set of a priori elements, obtained from the truth ephemeris of the 69-component SRP model, was used for all of the options. It is seen from Tables 3 and 4 that the option of using the Earth-pointing plate alone gives the

TABLE 3. DIFFERENCES BETWEEN THE FINAL AND A PRIORI ELEMENTS
(FINAL MINUS A PRIORI)

| CHANGES IN ELEMENTS | RUN CONFIGURATION | | | | |
|---------------------------|--|--|--|--|--|
| | CONSTANT EFFECTIVE AREA SOLVED FOR | TWO-PLATE MODEL α_E AND α_S SOLVED FOR | TWO-PLATE MODEL ξ_1 AND ξ_2 SOLVED FOR | TWO-PLATE MODEL ξ_3 AND ξ_4 SOLVED FOR | TWO-PLATE MODEL $\xi_1, \xi_2,$ AND ξ_3 SOLVED FOR |
| ΔX (meters) | -5.81 | -3.42 | -24.16 | -1.62 | -2.63 |
| ΔY (meters) | -12.62 | -9.57 | -18.43 | -8.59 | -7.61 |
| ΔZ (meters) | -24.80 | 16.07 | -109.73 | -38.56 | 11.17 |
| $\Delta \dot{X}$ (cm/sec) | 0.052 | 0.036 | 0.250 | 0.008 | 0.029 |
| $\Delta \dot{Y}$ (cm/sec) | -0.041 | -0.024 | -0.221 | -0.005 | -0.025 |
| $\Delta \dot{Z}$ (cm/sec) | -0.118 | -0.138 | 0.243 | -0.141 | -0.084 |

8316/81

- NOTES: 1. THE SAME SET OF A PRIORI ELEMENTS WAS USED FOR ALL DC PROGRAM RUNS.
2. THE QUANTITIES α_E AND α_S DENOTE SCALE FACTORS FOR THE AREAS OF THE EARTH-POINTING PLATE AND THE SOLAR PLATE, RESPECTIVELY. THE PARAMETERS $\xi_1, \xi_2, \xi_3,$ AND ξ_4 ARE DEFINED AS FOLLOWS: $\xi_1 = \alpha_E \eta_E, \xi_2 = \alpha_E (1 - \eta_E), \xi_3 = \alpha_S \eta_S,$ $\xi_4 = \alpha_S (1 - \eta_S),$ WHERE η_E AND η_S DENOTE THE REFLECTIVITY OF THE EARTH-POINTING PLATE AND THE SOLAR PLATE, RESPECTIVELY.

TABLE 4. DC PROGRAM STATISTICS AND SRP PARAMETERS SOLVED FOR

| PARAMETERS | RUN CONFIGURATION | | | | |
|------------------------------|--|---|---|---|--|
| | CONSTANT EFFECTIVE AREA SOLVED FOR | TWO-PLATE MODEL α_E AND α_S SOLVED FOR | TWO-PLATE MODEL ξ_1 AND ξ_2 SOLVED FOR | TWO-PLATE MODEL ξ_3 AND ξ_4 SOLVED FOR | TWO-PLATE MODEL $\xi_1, \xi_2, \text{ AND } \xi_3$ SOLVED FOR |
| WEIGHTED RMS | 0.0558 | 0.0346 | 0.3238 | 0.0546 | 0.0329 |
| STANDARD DEVIATION | | | | | |
| RANGE (meters) | 0.514 | 0.584 | 2.206 | 0.481 | 0.593 |
| DOPPLER (millihertz) | 0.914 | 0.473 | 5.416 | 0.898 | 0.431 |
| SRP PARAMETERS SOLVED FOR | $C_R = 1.38$ | $\alpha_E = 0.281$ $\alpha_S = 1.219$ | $\xi_1 = 1.971$ $\xi_2 = 0.551$ | $\xi_3 = 19.482$ $\xi_4 = -37.588$ | $\xi_1 = 0.175$ $\xi_2 = 0.146$ $\xi_3 = 0.602$ |

poorest results, whereas the other options all give comparable results. Similar conclusions are supported by Figures 2 and 3, which represent 24-hour ephemeris comparison results between the original 69-component ephemeris and the ephemerides obtained using the DC Program solutions for different SRP options. The results obtained using the second option, in which α_E and α_S were solved for, are not shown because they are very similar to the results obtained using the fourth option. Only the along-track and cross-track position differences are shown in Figures 2 and 3, because the radial position differences were much smaller than the along-track or cross-track position differences.

The single-plate option using the Earth-pointing plate alone gives the worst position errors. The single-plate option using the solar plate alone gives significantly better results. In fact, the option using the solar plate alone gives the smallest along-track position differences of all the different options used.

There are two features worth mentioning. First, there is no significant difference between the constant-effective-area model and the more complex two-plate model options. Second, in all cases studied, there are quite sizable cross-track position differences, equal to or larger than the along-track differences.

In order to examine the influence of the tracking geometry on the orbit determination results, a different pair of ground transponders (Rosman and Santiago) was used for the same series of DC Program solutions discussed above. Ephemeris comparison results obtained using these differential correction solutions were then compared with the corresponding results obtained using the pair of ground transponders at Rosman and Mojave; the only significant difference between

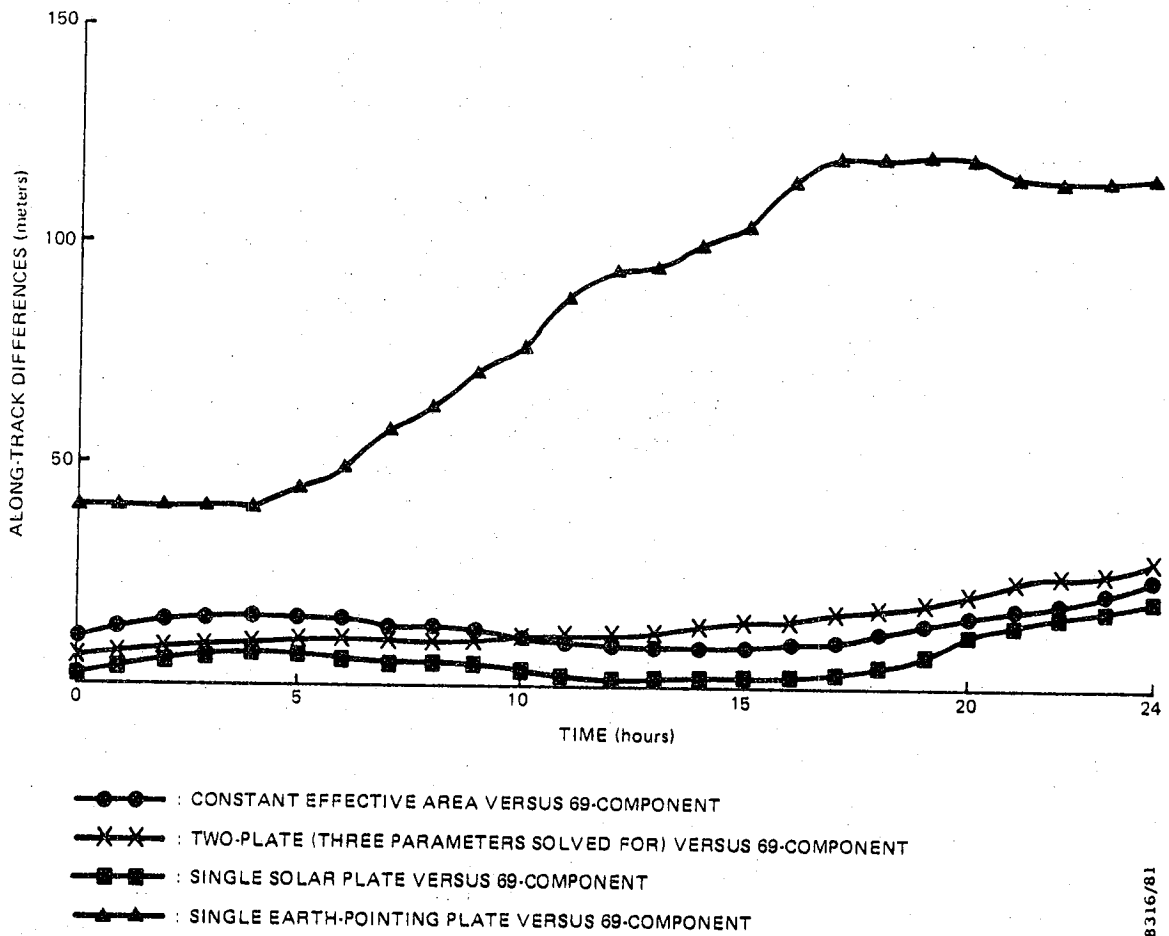
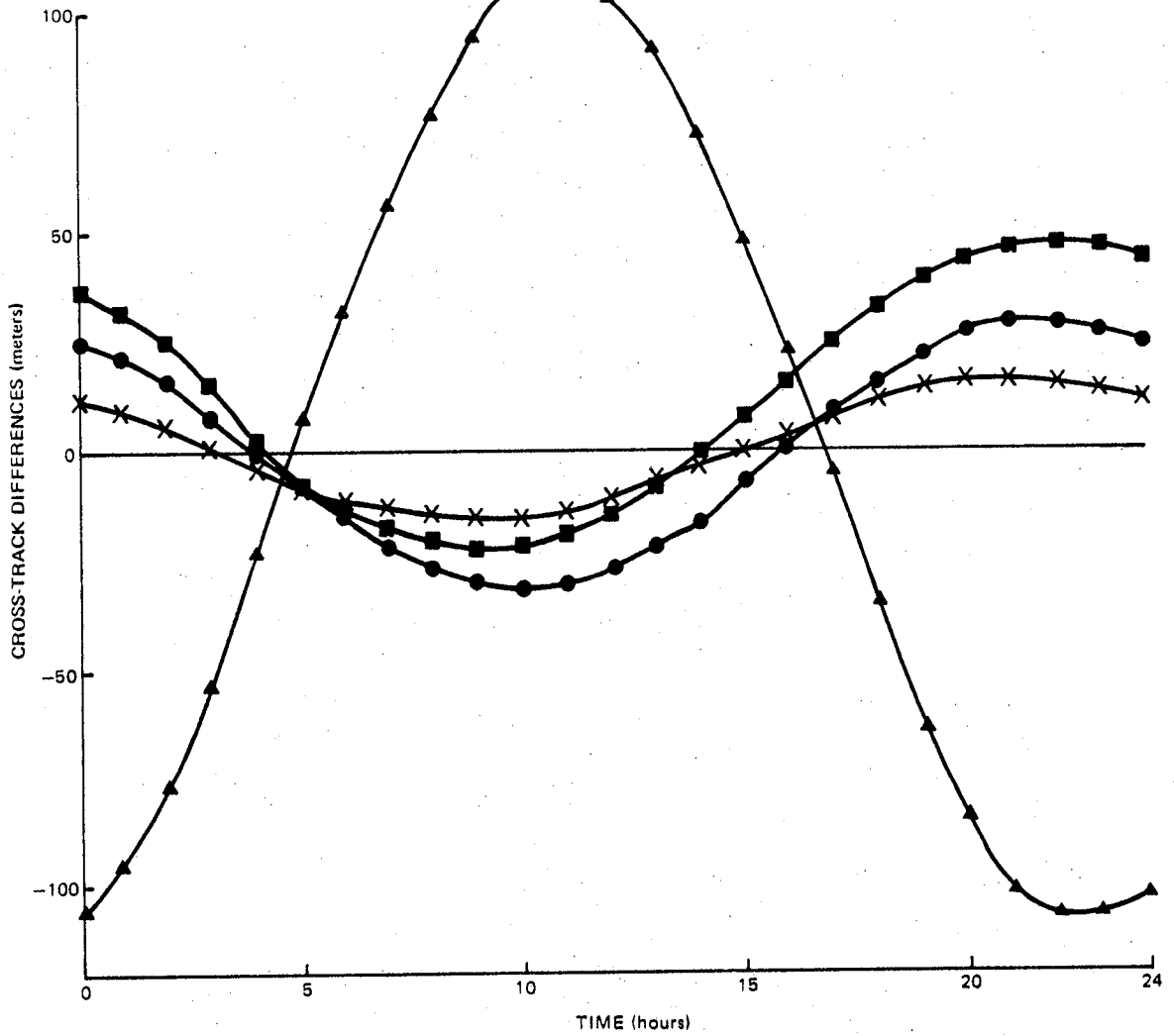


FIGURE 2. ALONG-TRACK POSITION DIFFERENCES FROM 24-HOUR EPHEMERIS COMPARISON RESULTS

8316/81



- : CONSTANT EFFECTIVE AREA VERSUS 69-COMPONENT
- ×× : TWO-PLATE (THREE PARAMETERS SOLVED FOR) VERSUS 69-COMPONENT
- ■ : SINGLE SOLAR PLATE VERSUS 69-COMPONENT
- ▲▲ : SINGLE EARTH-POINTING PLATE VERSUS 69-COMPONENT

FIGURE 3. CROSS-TRACK POSITION DIFFERENCES FROM 24-HOUR EPHEMERIS COMPARISON RESULTS

8316/81

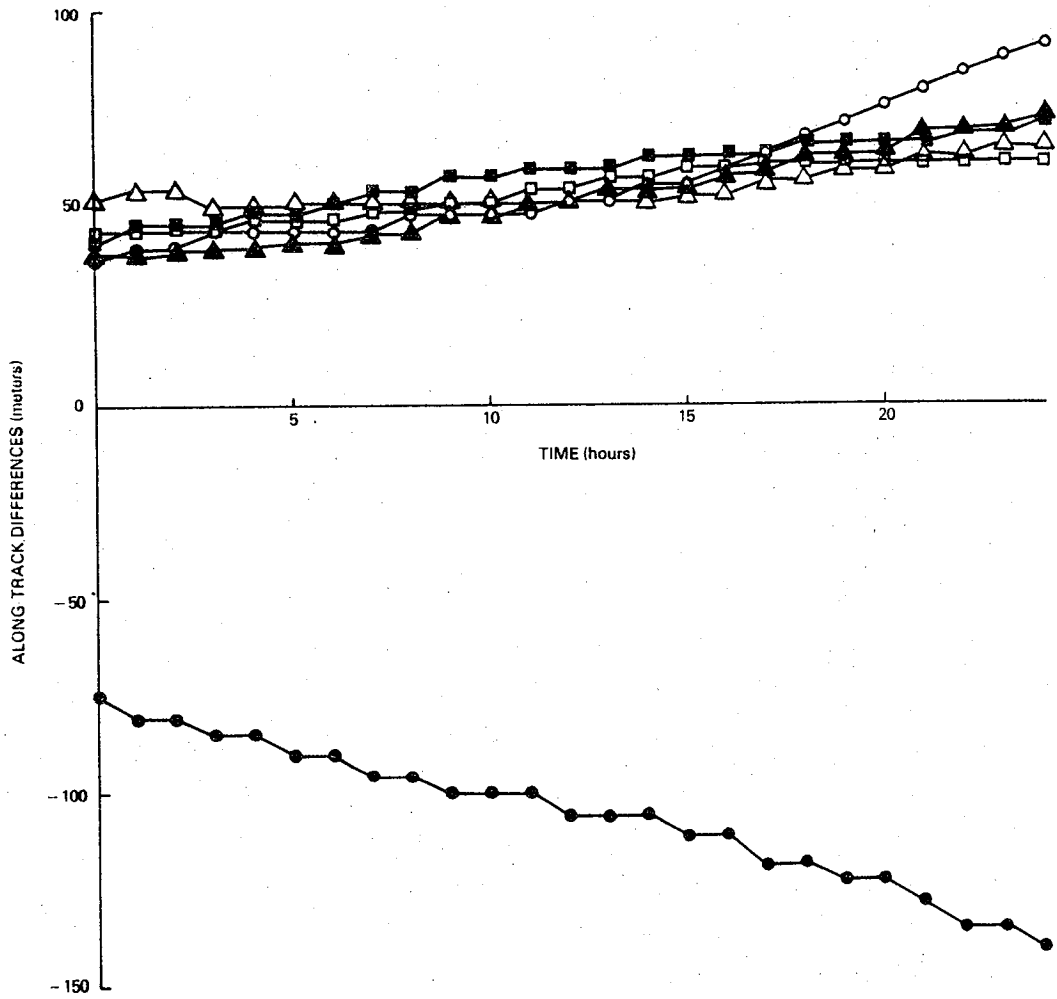
the two sets of results was in the cross-track position differences. The maximum cross-track position differences obtained using the Rosman and Santiago ground transponders were found to be less than 10 meters, whereas the corresponding differences obtained using the Rosman and Mojave ground transponders were larger than 20 meters.

4.2 RESULTS OBTAINED USING S-BAND RANGE DATA AND TWO GROUND TRACKING STATIONS

Differential correction solutions for a 24-hour TDRS arc were obtained using S-Band range data and two different tracking station configurations. In the first set of solutions, the two ground stations at Rosman and Mojave were used, and in the second set of solutions, the two stations at Rosman and Santiago were used. The results of 24-hour ephemeris comparisons are summarized in Figures 4 and 5. It is seen from Figures 4 and 5 that the results obtained using S-Band range data are generally worse than the corresponding results obtained using bilateration data. The along-track position differences shown in Figure 4 indicate that the Rosman/Mojave configuration gives somewhat better results than does the Rosman/Santiago configuration. In the case of the cross-track position differences shown in Figure 5, the situation is reversed; the Rosman/Santiago configuration gives somewhat better results than does the Rosman/Mojave configuration.

4.3 RESULTS OBTAINED USING MORE THAN TWO GROUND TRACKING STATIONS

The same 24-hour TDRS arc studied in Sections 4.1 and 4.2 was used in a set of DC Program runs using more than two ground tracking facilities. In the case of bilateration data, three ground transponders, located at Mojave, Santiago, and Madrid, and five ground transponders, located at Mojave, Santiago, Madrid, Rosman, and Quito, were used. Ephemeris

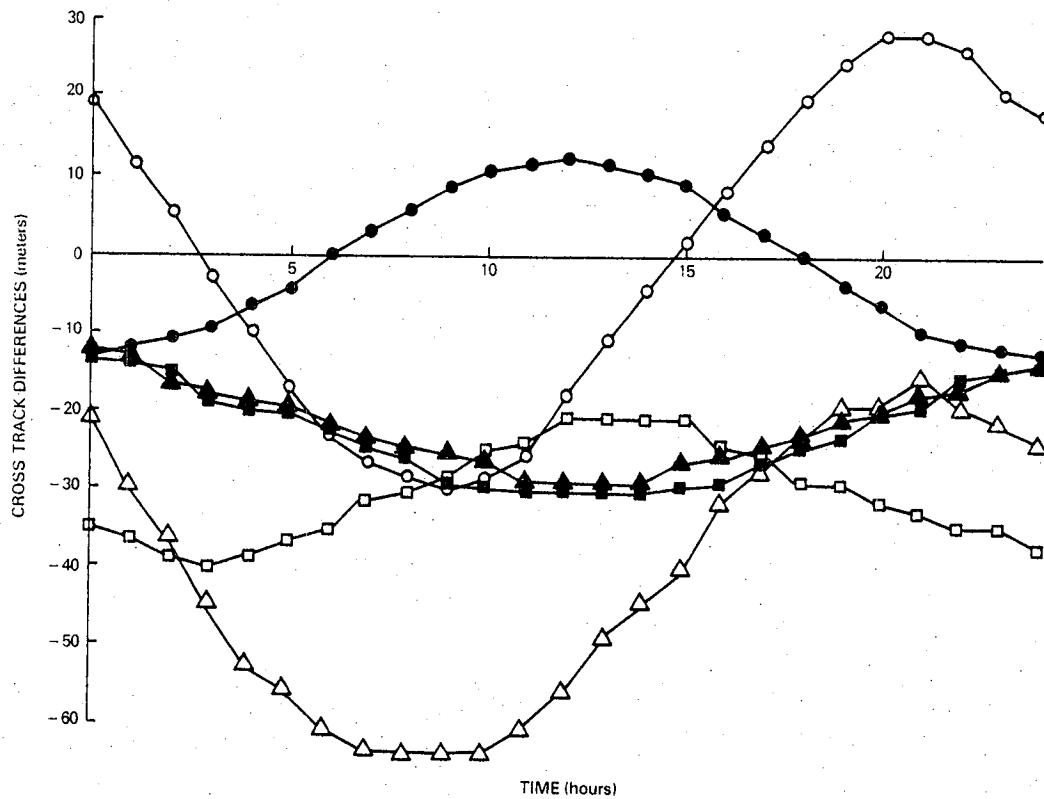


TRACKING CONFIGURATION

- | | | |
|----------|----------|--|
| ROS, GDS | ROS, AGO | |
| ○—○ | ●—● | : CONSTANT-EFFECTIVE-AREA vs 69-COMPONENT |
| □—□ | ■—■ | : TWO-PLATE (ξ_3 AND ξ_4 SOLVED FOR) vs 69-COMPONENT |
| △—△ | ▲—▲ | : TWO-PLATE ($\xi_1, \xi_2, \xi_3,$ AND ξ_4 SOLVED FOR) vs 69-COMPONENT |

FIGURE 4. ALONG-TRACK POSITION DIFFERENCES FROM 24-HOUR EPHEMERIS COMPARISON RESULTS

8347/81



TRACKING CONFIGURATION

- | | | | |
|----------|----------|---|--|
| ROS, GDS | ROS, AGO | : | CONSTANT-EFFECTIVE-AREA vs 69-COMPONENT |
| □ | ■ | : | TWO-PLATE (ξ_3 AND ξ_4 SOLVED FOR) vs 69-COMPONENT |
| △ | ▲ | : | TWO-PLATE ($\xi_1, \xi_2, \xi_3,$ AND ξ_4 SOLVED FOR) vs 69-COMPONENT |

8347/81

FIGURE 5. CROSS-TRACK POSITION DIFFERENCES FROM 24-HOUR EPHEMERIS COMPARISON RESULTS

comparison results obtained using the three ground transponders were similar to the results obtained using the five ground transponders. Typical along-track, cross-track, and radial position differences were 6.0, 1.0, and 1.0 meters, respectively. No significant difference was found among the different models used for the solar radiation pressure computation as long as the initial state vector and the solar radiation pressure parameters were solved for.

Similar analyses were carried out using more than two S-Band tracking stations. Two sets of differential correction solutions were obtained using three tracking stations at Mojave, Madrid, and Santiago and four tracking stations at Mojave, Rosman, Madrid, and Santiago. Ephemeris comparison results obtained using these differential correction solutions are summarized in Tables 5 and 6. There is no essential difference between the results obtained using three tracking stations and the results obtained using four tracking stations. These results show a significant improvement over the corresponding results obtained using only two S-Band tracking stations. Cross-track position differences were reduced by almost a factor of 10 and along-track differences were also substantially reduced. However, none of the results obtained using S-Band tracking data were as good as the corresponding results obtained using bilateration data.

TABLE 5. CROSS-TRACK AND ALONG-TRACK POSITION DIFFERENCES OBTAINED
USING THREE USB GROUND STATIONS (MAD, AVE, AGO)

| EPHEMERIDES COMPARED | MAXIMUM CROSS-TRACK DIFFERENCE (meters) | MAXIMUM ALONG-TRACK DIFFERENCE (meters) |
|--|--|--|
| CONSTANT-EFFECTIVE-AREA vs 69-COMPONENT | 3.1 | 24.6 |
| TWO-PLATE (α_E AND α_S SOLVED FOR) vs 69-COMPONENT | 2.8 | 23.5 |
| SINGLE SOLAR PLATE (ξ_3 AND ξ_4 SOLVED FOR) vs 69-COMPONENT | 7.1 | 22.2 |
| TWO-PLATE ($\xi_1, \xi_2, \xi_3,$ AND ξ_4 SOLVED FOR) vs 69-COMPONENT | 6.5 | 20.2 |

**TABLE 6. CROSS-TRACK AND ALONG-TRACK POSITION DIFFERENCES OBTAINED
USING FOUR USB GROUND STATIONS (MAD, AVE, AGO, ROS)**

| EPHEMERIDES COMPARED | MAXIMUM CROSS-TRACK DIFFERENCE (meters) | MAXIMUM ALONG-TRACK DIFFERENCE (meters) |
|--|--|--|
| CONSTANT-EFFECTIVE AREA vs 69-COMPONENT | 3.3 | 26.2 |
| TWO-PLATE (α_E AND α_S SOLVED FOR) vs 69-COMPONENT | 3.2 | 25.9 |
| SINGLE SOLAR PLATE (ξ_3 AND ξ_4 SOLVED FOR) vs 69-COMPONENT | 4.4 | 26.7 |
| TWO-PLATE ($\xi_1, \xi_2, \xi_3,$ AND ξ_4 SOLVED FOR) vs 69-COMPONENT | 4.2 | 25.0 |

SECTION 5 - CONCLUSIONS

A study of solar radiation pressure (SRP) as it affects TDRS orbits was performed using simulated bilateration data, simulated direct two-way data, and various ground station configurations. Orbit determination results obtained using constant-effective-area and two-plate SRP modeling were compared with each other and with an ephemeris obtained using a 69-component TDRS SRP model. The conclusion of this study can be summarized as follows:

- The constant-effective-area solar radiation pressure model and the two-plate model give essentially the same quality results when both the state and the SRP parameters are solved for. The maximum position differences between the 69-component model truth ephemeris and an ephemeris determined using solved-for elements and SRP parameters can be reduced to less than 10 meters if proper bilateration tracking configurations are used in solving for the elements and the SRP parameters.
- When using only two ground tracking facilities, the Rosman/Santiago combination gives smaller cross-track position errors than does the Rosman/Mojave combination.
- Results obtained using three ground tracking facilities (located in a triangular configuration) are significantly better than the corresponding results obtained using two ground tracking facilities.
- Results obtained using more than three ground tracking facilities are of essentially the same

quality as the results obtained using three ground tracking facilities.

- Bilateralation data appear to give better orbit determination results than S-Band tracking data.

REFERENCES

1. Systems and Applied Sciences Corporation, Feasibility Study of Using a Two-Plate Model to Approximate the Tracking and Data Relay Satellite, F. K. Chan, M. H. Toporek, and J. R. Bohse, August 1979
2. Computer Sciences Corporation, CSC/TM-80/6030, Task 758 Final Report, R. E. Shanklin et al., October 1980
3. Goddard Space Flight Center, X-582-76-77, Mathematical Theory of the Goddard Trajectory Determination System (GTDS), J. O. Cappelleri, Jr., C. E. Velez, and A. J. Fuchs (editors), April 1976